

# Potential jump on a laser target

Yu A Bykovskii, I Yu Konyukhov, V D Peklenkov

**Abstract.** Various mechanisms of the appearance of a potential jump on a target irradiated by 10.6- $\mu\text{m}$  laser pulses in vacuum are considered. It is shown that, in principle, the potential jump can be used to monitor the parameters of the laser pulses and measure the electron temperature of a laser plasma.

**Keywords:** laser plasma, electron temperature, potential.

## 1. Introduction

Laser plasma has been studied as an ion source, with the results being applied to the development of laser ion sources for accelerators, neutron generators, the purposes of laser implantation, etc. The electron emission of laser plasma at early stages of its expansion in vacuum has been studied less well. Among other things, this emission leads to the formation of a double layer at the plasma boundary and the resulting change in the potential of the laser target [1–4]. The mechanisms of the appearance of electric fields during the optical breakdown of air were presented in detail in Refs [5–7].

These questions are of interest because laser plasma can be used to create pulsed sources of current, which, for example, can power solenoids that produce strong magnetic fields  $\sim 100$  T [8]. Attempts have been made to relate the measurable characteristics of the electron emission with one of the most important parameters of laser plasma — the electron temperature  $T_e$  [9–11]. In our opinion, this problem is particularly important because, at present, there are no simple universal methods for monitoring  $T_e$  in laser-plasma facilities. Apart from practical applications, studies of the electron emission characteristics of laser plasma have an important fundamental aspect, namely, the investigation of the formation of the double layer at the plasma boundary, which significantly affects the energy spectra of multiply charged ions in laser plasma [12].

The purposes of this work are to study the correlation between the laser pulse and the potential jump  $V$  on the laser target and to investigate how the potential jump de-

pends on the parameters of the laser radiation, the characteristics of the vacuum, and other physical conditions. Based on the results obtained, we develop a technique for monitoring the laser flux density on the target surface with the help of measurements of  $V$  and study the possibility of developing a technique for monitoring the electron temperature  $T_e$  of plasma.

## 2. Experimental setup

Fig. 1 shows the scheme of the experimental setup. We used a pulsed transverse-discharge  $\text{CO}_2$ -laser 1. A laser pulse had a profile typical for high-pressure  $\text{CO}_2$ -lasers: a giant pulse with a FWHM of 100–200 ns was followed by the radiation of lower intensity with the decay time of 5  $\mu\text{s}$ . With the help of deflecting mirrors 2 and 3, a laser beam was directed into a vacuum chamber 4 through an input window 5. The chamber contained a NaCl focusing lens 6 with a focal distance of 45 mm and a target 7. The maximum intensity  $\Phi$  of the focused radiation was  $2 \times 10^9$   $\text{W cm}^{-2}$ . A  $6 \times 6$ -cm brass plate 8 (electrode) was placed between the target and the lens, at a 2-cm distance from the target. The plate had a hole of diameter 5 mm in its centre to let the laser beam pass through. The target and the plate were

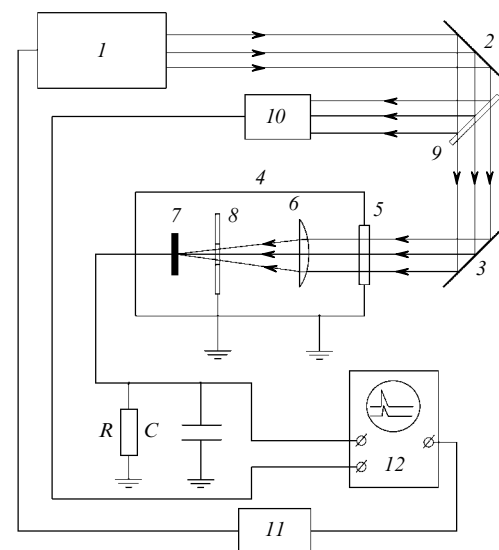


**Figure 1.** Scheme of the experimental setup: (1) laser, (2, 3) deflecting mirrors, (4) vacuum chamber, (5) input window, (6) focusing lens, (7) target, (8) brass plate (electrode), (9) beamsplitter, (10) FP-3 photodetector, (11) G5-15 pulse generator, (12) S8-I2 oscillograph.

Yu A Bykovskii, I Yu Konyukhov, V D Peklenkov Moscow State Engineering Physics Institute (Technical University), Kashirskoe sh. 31, 115409 Moscow, Russia

Received 30 May 2000

Kvantovaya Elektronika 31(1) 45–49 (2001)

Translated by I V Bargatin

isolated from the chamber walls, which were grounded in the experiment. This allowed us to measure the potential jump on both the target and the brass electrode. During these measurements, we grounded one of the electrodes and connected the other one to a  $RC$  circuit, whose output was fed to an oscillograph. The vacuum chamber was a  $20 \times 30 \times 60$ -cm rectangular parallelepiped made of stainless steel; the targets were made of C, Zr, Ta, and Pb. To study the correlation between the temporal dependence of the laser intensity and that of the target (electrode) potential, we employed a beam-splitter 9 and a photodetector 10. A two-beam storage oscillograph 12 recorded the photodetector output and the target (electrode) signal. A pulse generator 11 synchronised the start of the laser and the oscillograph.

### 3. Experimental results

At the first stage of the experiments, we studied how the potential jump on the laser target depends on the laser radiation intensity and investigated the nature of the potential jump itself. In these experiments, the target was connected to the resistor  $R = 1$  M $\Omega$  and the capacity  $C = 100$  pF (a parasitic capacity), and the electrode was grounded. The system was evacuated to  $(2 - 3) \times 10^{-5}$  Torr.

Fig. 2 shows typical oscillograms of the potential jump on the target and a laser pulse. The shape of the signal from the target was independent of the target material and was similar to the laser pulse shape. The pulse of the target potential was positive; it had a single peak, a steep (100-ns) leading edge, and a slowly decaying trailing edge (with a decay time of 10  $\mu$ s). The experiments have shown that the onset of the laser pulse coincided with the onset of the variation in the target potential. A weak modulation observed in the tails of the pulses was due to the noise pickup.

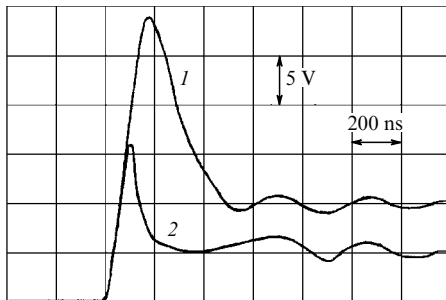


**Figure 2.** Oscillograms of the potential jump on the laser target (1) and the laser pulse (2) for  $R = 1$  M $\Omega$ ,  $C = 100$  pF, and the grounded electrode.

Fig. 3 shows experimental dependences of the potential jump  $V$  on the laser radiation intensity  $\Phi$  in the logarithmic scale. We changed the intensity  $\Phi$  with the help of calibrated filters with the attenuation coefficient  $K = 1.36$ . The diameter of the focal spot remained constant and equal to 300  $\mu$ m. One can see that, regardless of the target material, the potential jump on the laser target increases monotonically with increasing  $\Phi$ . Note that the appearance of the potential jump exhibited a threshold behaviour: if  $\Phi$  was reduced below the plasma formation threshold, the target signal fell off dramatically by more than one order of magnitude. We inferred the plasma formation threshold from the disappearance of the ion current from the electrode, which

was used in our experiments as a collector, while the target was grounded. Thus, we can assume that neither thermal emission nor photoemission from the target surface seriously affect the potential jump of the target.

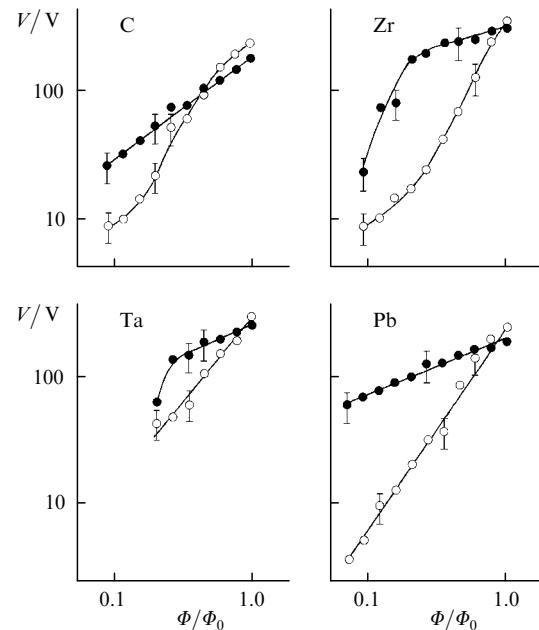


**Figure 3.** Dependences of the potential jump  $V$  on the C, Zr, Ta, and Pb targets on the laser radiation intensity  $\Phi$  for  $\Phi_0 = 2 \times 10^9$  W cm $^{-2}$ , the pressures  $2 \times 10^{-5}$  ( $\circ$ ) and  $2 \times 10^{-2}$  Torr ( $\bullet$ ), and the grounded electrode.

The potential jump on the laser target could also be caused by the secondary emission of electrons from the target surface under the action of plasma-produced X-rays and UV radiation. To find out whether the secondary electron emission actually affected the target potential, we performed a special experiment. The target surface was covered by a thin (0.5-mm) layer of organic glass, which was opaque for the laser radiation. This shield should strongly reduce the secondary emission caused by the plasma-produced radiation.

In the experiment, we observed no variation in the target potential until the laser beam burned through the organic glass plate. After that, we observed a signal from the target whose principal part had the amplitude and shape that coincided to within 30% with the corresponding characteristics obtained in the absence of the plate. We may then conclude that, under these experimental conditions, the plasma-produced secondary electron emission from the target surface does not significantly affect the observed potential jump of the target. This conclusion agrees with the results of Ref. [10], where it was shown that in the case of micro-targets and the laser intensity  $\Phi = 10^{14}$  W cm $^{-2}$  neither of the mentioned mechanisms was responsible for the potential jump.

Therefore, the only reasonable explanation of the appearance of the potential jump is the escape of electrons from the plasma bunch and the formation of a double layer on the plasma boundary, which consists of an external electron cloud and a bordering electron-depleted plasma layer. This spatial separation of the charge is caused by the difference between the masses of electrons and ions [12]. The

presence of the electron emission from the plasma bunch was confirmed experimentally. If the target signal was positive, then in the case of the grounded target, the electrode signal was negative, indicating the charge separation. The experiment (Fig. 4) shows that, in the case of the grounded target and  $R = 1$  MOhm, the dependence on  $\Phi$  of the modulus of the electrode potential jump  $|V_e|$  ( $V_e < 0$ ) is similar to the target's dependence  $V(\Phi)$  observed in the case of the grounded electrode (Fig. 3).

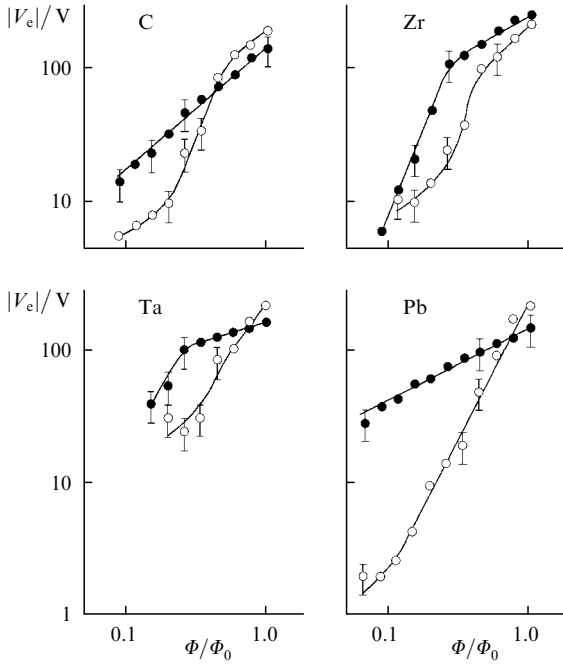


**Figure 4.** Dependences of the modulus of the electrode potential jump  $|V_e|$  ( $V_e < 0$ ) on the laser radiation intensity  $\Phi$  in the case of the grounded C, Zr, Ta, and Pb targets at pressures  $2 \times 10^{-5}$  (○) and  $2 \times 10^{-2}$  Torr (●).

However the authors of paper [7], who studied the plasma electric fields near various targets during the optical breakdown in air, believe that the double layer is formed due to the gradients of the electron density and the temperature inside the plasma. By compensating this charge separation, the electromagnetic forces generate double layers in plasma bunches (opposite dipole moments appear at the leading and trailing edges of the plasma). The conducting target removes the dipole at the trailing edge because any potential difference created in the plasma due to the charge separation connects up to the metal surface. Therefore, the double layer is induced by the dipole at the leading edge of the plasma, resulting in the negative potential in front of the target. However, if we assume that the temperature gradient in the plasma is insignificant, so that the plasma can be characterised by some average electron temperature, then the charge separation at the leading edge of the plasma expanding in the vacuum is caused by the difference between the masses of electrons and ions.

A theoretical model describing the appearance of the potential jump  $V$  on a target caused by the electron emission from the plasma bunch was developed in Ref. [9]. In the case of an isolated target having the capacitance  $C$  with respect to the electrode (in our case, this electrode was the chamber walls), we obtain

$$V = eN_0(eV)^{1/2} \left( 1 + \frac{kT_e}{2eV} \right) \times \exp \left( -\frac{eV}{kT_e} \right) \frac{1}{C(\pi kT_e)^{1/2}}, \quad (1)$$

where  $N_0$  is the total number of electrons in the plasma,  $e$  is the elementary charge, and  $k$  is the Boltzmann constant. Expression (1) was derived by assuming that all electrons whose energy exceeds  $eV$  reached the chamber walls. In this way, the capacitance  $C$  is charged to potential  $V$ , when all electrons become Maxwellian and the influence of the double layer of the plasma boundary can be neglected.

The calculation by expression (1) for  $N_0/C$  fixed, gives the dependence  $V(T_e)$ , which is close to  $V \sim T_e$ . The potential jump  $V$  only weakly depends on the ratio  $N_0/C$ : when  $N_0/C$  increases from  $10^{27}$  to  $10^{29}$ , the potential  $V$  increases less than twice. According to Refs [13, 14],  $T_e \sim \Phi^{4/9}$  or  $\Phi^{2/3}$  depending on the experimental conditions; therefore, the potential  $V$  should be proportional to  $\Phi^{4/9-2/3}$ . However, we observed (Figs 3 and 4) a stronger dependence  $V \sim \Phi^\alpha$ , where  $1 \leq \alpha \leq 2$  depending on the atomic weight of the target material.

At the same time, the analysis of the potential jump oscillograms and their correlation with the laser pulse (Fig. 2) shows that there is a time delay between the maximum of  $V$  and the maximum of  $\Phi$  which increases with increasing radiation intensity. The maximum of  $V$  is observed later than the maximum of  $\Phi$ . This time delay can be easily explained if we assume that  $V < \phi$ , where  $\phi$  is the potential difference at the double layer. In this case, a potential well for electrons forms between the plasma boundary and the electrode, limiting the charging current of the capacitance  $C$ . Assuming that the electrons follow the Maxwell–Boltzmann energy distribution and neglecting the leakage current, we obtain

$$V = j_e \exp \left( -\frac{e\phi}{kT_e} \right) \tau \frac{S}{C}, \quad (2)$$

where  $j_e = en_e(2kT_e/\pi m_e)^{1/2}/2$  is the density of the thermal electron current,  $m_e$  is the electron mass,  $e\phi$  is the depth of the potential well of the double layer for electrons,  $\tau$  is the laser pulse duration,  $n_e$  is the electron density, and  $S$  is the area of the plasma surface. Assuming that  $S$  coincides with the focal spot area and taking into account that  $T_e \sim \Phi^{4/9-2/3}$ ,  $n_e = Zn_i$  (due to the quasi-neutrality of the plasma), where the average ion charge  $Z = 1$ , and  $n_i \sim N_i \sim \Phi^{0.9-1.1}$ , where  $N_i$  is the total number of ions in the plasma, we obtain  $V \sim \Phi^{\alpha_{th}}$  ( $1.1 \leq \alpha_{th} \leq 1.4$ ) for  $\Phi$  near the plasma formation threshold [15]. In these estimates, the upper limit is undervalued because  $S$  actually increases with increasing  $\Phi$ . In the case of a two-dimensional geometry and  $S \ll \pi \tau^2 kT_e/2m_i$  (where  $m_i$  is the ion mass), we have  $T_e \sim \Phi^{4/9-2/3}$ . This yields the upper limit  $\alpha_{th} \sim 2$ , which well agrees with the experiment.

Thus, we can conclude from the above analysis that, when the laser radiation intensity is close to the plasma formation threshold, the detected potential jump on the laser target (electrode) can strongly depend on the presence of the double layer at the plasma boundary. Although the obtained results are rather difficult to interpret, our experiment has shown that there is a one-to-one correspondence between the intensity  $\Phi$  and the potential  $V$ :  $V$  increases monotonically with increasing  $\Phi$ .

Fig. 5 shows the experimentally measured  $V$  in the case when the laser beam was defocused but its energy (power) remained unchanged. The beam was defocused by longitudinal displacement of lens 6 (Fig. 1) in both directions. The focal plane of the lens then shifted correspondingly by a distance  $L$ . One can see from Fig. 5 that, regardless of the target material, the maximum  $V$  is reached for the minimum focal spot size or the maximum  $\Phi$ . We believe that these results are of great importance because they allow a simple method for monitoring  $\Phi$  in laser-plasma setups.

It would be of interest to employ the potential jump measurements for monitoring parameters of the laser plasma and, in particular, for monitoring one of its most important parameters – the electron temperature. Formula (2) is hardly suitable for this purpose because it depends on

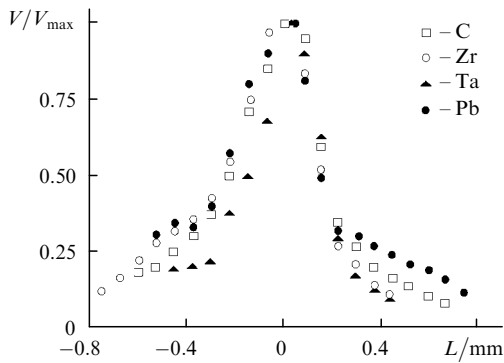


**Figure 5.** Dependences of the relative variation in the potential jump  $V/V_{\max}$  on the target on the distance  $L$  to the focal plane for various target materials and the grounded electrode.

many parameters, including the physical conditions of the plasma formation and expansion, which cannot be easily expressed analytically. In this connection, we believe it is more promising to search for methods of measuring the potential difference  $\varphi$  of the double layer, which should primarily depend on the parameters of the plasma itself. This potential difference can be defined as the floating plasma potential assuming that the electron and ion currents flowing through the double layer are equal (similarly to the case of electric probes [16]):

$$\varphi = \frac{1}{2} kT_e \ln \frac{2m_i}{\pi m_e}.$$

In the case of the ion atomic weight  $A = 12 - 200$ , we have  $kT_e \approx (0.16 - 0.2)\varphi$ . A more rigorous theoretical analysis of the dependence  $\varphi(T_e)$  for the laser plasma (neglecting its expansion) gave the relation  $kT_e \sim 0.2\varphi$  [17].

It was shown in Ref. [18] that the electron current from the target to the electrode can be increased by increasing the pressure in the vacuum chamber to  $10^{-2}$  Torr, thereby producing a background plasma in the space between the target and the electrode. This is equivalent to connecting a low resistance between the negative component of the double layer and the electrode. Based on these results, we expected that under our experimental conditions the capacitance  $C$  could be charged to the maximum possible potential  $\varphi$  by degrading the vacuum to  $10^{-2}$  Torr.

Figs 3 and 4 show the experimental dependences of  $V$  and  $|V_e|$  on  $\Phi$  that were measured at a pressure of  $2 \times 10^{-2}$  Torr. In this case, the variations in the target potential and

the temperature agree to within experimental errors:  $V(\Phi) \sim \Phi^\alpha$ , where  $\alpha = 0.7$  for the carbon target and 0.5 for the Zr, Ta, and Pb targets. The deviation of the experimental curves from the theoretical ones near the plasma formation threshold could be caused by the partial reflection of the laser radiation from the metal surfaces of Zr and Ta. This is supported by the fact that, in the case of the carbon target, the dependence  $V(\Phi)$  exhibits no anomaly until the plasma formation threshold. In the case of the Pb target, the intensities used are much higher than the plasma formation threshold.

Fig. 6 shows the dependence of the electron temperature of the laser plasma on the parameter  $\lambda^2\Phi$ , where  $\lambda$  is the laser radiation wavelength. We plotted this curve by combining various experimental results presented in review [14]. Fig. 6 also includes our own results of measuring  $T_e$  in the  $2 \times 10^{-2}$  Torr vacuum using the relation  $kT_e = (0.16 - 0.2)V$ , where the coefficient depends on  $A$ , as noted above. One can see that these results and the dependence of  $kT_e$  on  $\Phi$  presented in Ref. [14] are in a satisfactory agreement given  $kT_e$  is specified up to the coefficient  $(A/Z)^{1/3}$ . Despite this good agreement, the possibility of determining  $T_e$  from  $V$  with the help of the above relation needs to be substantiated by a more detailed physical study.

## 4. Conclusions

The results of our experiments and the analysis of other publications demonstrate that the appearance of the

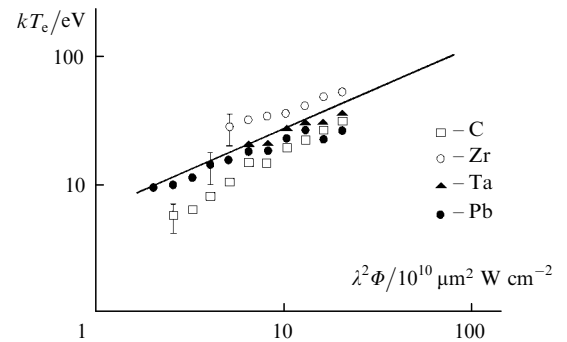


**Figure 6.** Dependences of  $kT_e$  on  $\lambda^2\Phi$  for various target materials in the case of the  $2 \times 10^{-2}$ -Torr vacuum and the grounded electrode, as well as the results presented in review [14] (the straight line).

potential jump on the laser target can be explained by the formation of a double layer because of the difference between the masses of electrons and ions. We have studied the dependence of the potential jump of the laser target on the laser radiation intensity and demonstrated that there is a one-to-one correspondence between these quantities. This allows for a simple method of monitoring the laser radiation parameters (its intensity and focal spot).

The proposed method of determining the electron temperature of the laser plasma from the potential jump on the laser target can significantly facilitate measurements of this important parameter of laser-plasma setups.

**Acknowledgements.** This work was supported by the Education-Science Centre ‘Fundamental Optics and Spectroscopy’ within the framework of the Federal Special Program ‘Integration’.

## References

1. Silfvast W T, Szeto L H *Appl. Phys. Lett.* **31** 726 (1977)
2. Mendel C W, Olsen J H *Phys. Rev. Lett.* **34** 859 (1975)
3. Antipov A A, Grasyuk A Z, Losev L L, Lutsenko A P, Meshal-kin E A *Fizika Plazmy* **13** 336 (1987) [*Sov. J. Plasma Phys.* **13** 191 (1987)]
4. Barkhudarov E M, Gelashvili G V, Gumberidze G G, Taktakish- vili M I *Fizika Plazmy* **10** 757 (1984) [*Sov. J. Plasma Phys.* **10** 439 (1984)]
5. Dement'ev D A, Konov V I, Nikitin P I, Prokhorov A M *Kvantovaya Elektron.* **8** 1532 (1981) [*Sov. J. Quantum Electron.* **11** 923 (1981)]
6. Kabashin A V, Nikitin P I *Kvantovaya Elektron. (Moscow)* **24** 551 (1997) [*Quantum Electron.* **27** 536 (1997)]
7. Kabashin A V, Nikitin P I, Marine W, Sentis M *Kvantovaya Elektron.* **25** 26 (1998) [*Quantum Electron.* **28** 24 (1998)]
8. Daido H, Mima R et al. *Phys. Rev. Lett.* **56** 846 (1985)
9. Peariman J S, Dahibacka G H *Appl. Phys. Lett.* **31** 414 (1977)
10. Benjamin R F, McCall G H, Ehler A W *Phys. Rev. Lett.* **42** 890 (1979)
11. Barkhudarov E M, Gelashvili G V, Gumberidze G G *XV Intern. Conf. on Phenomena in Ionised Bases* (Minsk, 1981) p. 207
12. Crow K E, Auer P L, Allen J E *Plasma Phys.* **14** 65 (1975)
13. Boiko V A, Krokhin O N, Sklizkov G V *Trudy FIAN* **76** 186 (1974)
14. Tonon G F *IEEE Trans. Nuclear Science* **19** 172 (1972)
15. Yamanato T, Munakata T, Nomiga Y et al. *Jap. J. Appl. Phys.* **23** 1337 (1984)
16. Huddleston R H, Leonard S L *Plasma diagnostic techniques* (New York: Academic, 1965)
17. Gurevich A V, Meshcherkin A P *Fizika Plazmy* **9** 955 (1983) [*Sov. J. Plasma Phys.* **9** 556 (1983)]
18. Barkhudarov E M, Gelashvili G V, Gumberidze G G *Fizika Plazmy* **12** 1489 (1986) [*Sov. J. Plasma Phys.* **12** 862 (1986)]